JOURNAL OF CATALYSIS **169,** 338–346 (1997)
ARTICLE NO. CA971709

γ-Alumina-Supported Pt Catalysts for Aromatics Reduction: A Structural Investigation of Sulfur Poisoning Catalyst Deactivation

J.-R. Chang,†,[1] S.-L. Chang,† and T.-B. Lin*

Chinese Petroleum Corporation, RMRC, Chia-Yi, Taiwan, Republic of China; and †Department of Chemical Engineering, National Chung Cheng University, Chia-Yi, Taiwan, Republic of China

Received November 1, 1996; revised March 27, 1997; accepted March 27, 1997

The effects of sulfur poisoning on the structural changes of γ-alumina-supported Pt catalysts were investigated by X-ray absorption spectroscopy and temperature-programmed reduction (TPR). Extended X-ray absorption fine structure (EXAFS) analysis of the fresh catalyst determined an average Pt–Pt coordination number of 2.6, suggesting an average platinum cluster size of 3 and 4 atoms formed on the γ-alumina surface. After the test reaction using a tetralin feed containing 1000 ppm sulfur at 270°C and 32 atm for 24 h, an increase of Pt cluster size was observed. A concomitant increase of the Pt–Pt coordination number to 7.3 with the formation of Pt–S contribution in EXAFS indicate that metal migration was induced by sulfur poisoning. The Pt–S contributions with bond distance of 2.34 and 2.53 Å were obtained by subtracting the Pt–Pt contribution from Fourier-isolated raw data. The results, combined with TPR peaks characterizing the sulfur-poisoned catalysts, suggest that the two Pt–S contributions were due to the interaction between Pt and the adsorbed H_2S and the formation of platinum sulfide (PtS). After the fresh catalysts were tested with more severe operation conditions (19 atm, 2000 ppm sulfur), the used catalysts were characterized by only one Pt–S contribution of bond distance 2.31 Å, indicating that clusters with a morphology closely resembling bulk PtS were formed on the surface. Based on the structural investigation results, we conclude that the loss of catalyst activity during sulfur poisoning is attributed to the adsorption of H_2S, sulfur-poisoning-induced Pt agglomeration and the formation of PtS.

INTRODUCTION

In order to meet gradually stricter diesel fuel standards (1), especially for aromatic content, refiners have been developing new processes to meet the challenge. Among them, a two-stage process, which uses a hydrotreating catalyst at the first reactor and a hydrogenation catalyst at the second, promises to achieve the required standard (2, 3). Two-stage processes normally use a supported-platinum catalyst for aromatics reduction. These catalysts exhibit excellent hydrogenation activity but are very sensitive to sulfur compounds in feed stock (4); hence a severe hydrotreating is necessary to reduce sulfur content in the feed to below 1 ppm. The application of the two-stage process is thus limited by such severe pretreatment conditions, unless the sulfur tolerance problems can be solved.

It has been determined that the sulfur resistance of a supported Pt catalyst can be enhanced by utilizing an acidic support, such as acidic zeolite (5), and by adding Pd to the Pt catalyst (6–12). However, notwithstanding the improvement, catalysts for aromatics reduction still suffer from low sulfur tolerance, and deep hydrodesulfurization is still necessary to reduce the sulfur content in diesel fuel (11). The retardation in improving the sulfur resistance of the supported Pt catalyst may be due to poor understanding of the fundamental chemistry involved in sulfur poisoning catalyst deactivation.

In a recent publication (13), we reported that the activity of sulfur-poisoned catalysts was unable to be fully recovered by hydrogen regeneration and the irreversibility was thought to be caused by the agglomeration of Pt particles, inferred from extended X-ray absorption fine structure analysis (EXAFS) characterizing the structure of the sulfur-poisoned Pt/BaK-LTL zeolite reported by Vaarkamp *et al.* (14), and from the EPMA (electron probe microanalysis) characterizing the Pt profile of the sulfur-poisoned Pt/γ-Al_2O_3 catalyst (13). The goal of this research was to confirm this inference by EXAFS spectroscopy, which has been shown to be useful for characterization of sulfur-poisoned Pt catalysts (14). In addition, together with results from the complementary characterization techniques, namely, EXAFS, temperature-programmed reduction (TPR), and EPMA, a possible mechanism was proposed to explain the Pt agglomeration induced by sulfur poisoning. Using this, the role of the acidic site in improving the sulfur resistance of a supported Pt catalyst was illustrated.

Tetralin hydrogenation was used as a model reaction to test the catalyst activity for aromatics reduction. Since the reaction can be carried out at low temperature (less than 270°C), catalyst deactivation caused by coke formation is relatively lower than that caused by sulfur poisoning.

---

[1] To whom correspondence should be addressed.

0021-9517/97 $25.00

Benzothiophene was chosen as the model compound for sulfur poisoning because (i) it is one of the sulfur compounds in diesel and (ii) its catalytic chemistry was fully understood (15).

EXPERIMENTAL

Materials and catalysts preparation. The catalyst samples were prepared by an impregnation technique. Alumina supports (A2U, γ-Al_2O_3, with a surface area of ~170 m^2/g and particle size of ~1.2 mm, purchased from Osaka Yogyo) were brought into contact with a solution of $[H_2PtCl_6]$ (Strem, 99.9%) in doubly distilled deionized water, followed with evacuation at room temperature, and then calcination at 450°C for 4 h. The catalyst sample contained 0.92 ± 0.02 wt% Pt, as measured by inductively coupled plasma optical emission spectroscopy with a Jarnell-Ash 1100 instrument. The sample was reduced at 450°C under 32 atm pure hydrogen (Sun-Fu, 99.99%) for 4 h, and it was reduced again at 300°C, 1 atm for 0.5 h, prior to the EXAFS measurement. This sample was noted as a fresh catalyst.

Tests of sulfur poisoning catalyst deactivation. The tests were carried out in a continuous downflow fixed-bed reactor. The reactor was a stainless-steel tube with an inside diameter of 1.2 cm. It was heated electrically and the temperature was controlled by a PID temperature controller with a sensor at the outer wall of the reactor. The temperature difference between the outer reactor wall and the center of the catalyst bed was about 15°C. The upstream part of the reactor was filled with particles of a catalytically inactive ceramic material for preheating and the inhibition of channeling effects.

The reaction system was first purged with dry nitrogen gas (Sun-Fu, 99.99%) for 2 h. Catalyst samples (sphere of 1.2 mm diameter) of 1.5 g (about 2 cc) were diluted with inert ceramic in a ratio of 1 : 5 (particle size about 200 μm) and then reduced at 450°C under 32 atm of pure hydrogen for 4 h. After reduction, the test was carried out with a weight hourly space velocity (WHSV) of 4.8 (g of feed/h · g of catalyst) with a hydrogen flow rate of 100 mL/min, at 270°C, under 32 atm total pressure for the normal sulfur poisoning test and at the same operating conditions but under 19 atm for the severe sulfur poisoning test.

Tetralin with 1000 ppm of sulfur was used as the feed for the normal sulfur poisoning test and 2000 ppm of sulfur for the severe one. Tetralin (Merck) was dried with particles of activated 4 Å molecular sieve and then was mixed with a certain amount of benzothiophene to prepare the feed.

The pump used in this study was a high-performance liquid chromatography pump (GL Science Inc., Model 576). As the pump employs a small double-plunger reciprocating pump which is controlled by a microprocessor, it can deliver a micro flow rate ranging from 0.001 to 9.99 mL/min.

Liquid products were trapped by a condenser at −5°C. Samples were collected periodically and analyzed by gas chromatography. The GC system used for feed and product analysis was a Shimadzu Model GC-14B gas chromatograph, equipped with a 10% OV-101 on Chrom W-HP 80/100 mesh column of 18 m × 0.22 mm i.d. and a flame ionization detector. The column was operated at 110°C with linear velocity 20 cm/min of dry nitrogen.

After the test reaction, the reactor was wetted with hexane at room temperature and 1 atm for 2 h, and then the catalysts were unloaded and grounded. The catalyst samples were then stored in nitrogen-filled sealed vials using a double manifold Schlenk vacuum line. Before the storage, the catalyst samples were exposed to air for about 0.5 h. As observed in the past, without hexane treatment the adsorbed oxygen may react with platinum clusters before EXAFS measurement (about 10 days) resulting in a formation of PtO_2. The function of the liquid hexane treatment of the catalysts is to protect the catalyst from exposure to air; the resistance to mass transfer of oxygen provided by hexane evidently minimizes the surface contamination by air during catalyst unloading and grounding.

The catalyst samples reacted at 32 and 19 atm and were noted as a normally sulfur-poisoned catalyst and a severely sulfur-poisoned catalyst, respectively. Prior to TPR and X-ray absorption spectroscopy measurement, the catalyst sample was purged with N_2 at room temperature for 1 h.

An H_2S adsorbed γ-Al_2O_3 sample for the TPR blank test was prepared by the adsorption of H_2S (Sun-Fu, 400 ppm H_2S in H_2, 250 mL) on 0.25 g γ-Al_2O_3 support at room temperature for 4 h.

Temperature-programmed reduction. The apparatus used for the TPR studies was described by Jones and McNicol (16). A gas stream of 10% H_2 in argon passed through the fresh and used catalysts in a quartz reactor heated at 10°C/min to 700°C with a temperature-programmed furnace. The amounts of H_2 consumed and off gas evolved in reduction were detected with a thermal conductivity detector. Any hydrocarbon compounds contained in the evolved gas were further identified by GC-14B gas chromatography with a 10% OV-101 column and an FID detector; sulfur compounds were identified by a SPB-1 sulfur (Supelco) column with a flame photometric detector. The reduction temperature was monitored by a thermocouple.

X-ray absorption spectroscopy. The X-ray adsorption measurements were performed on X-ray beamline X-11A of the National Synchrotron Light Source at Brookhaven National Laboratory with a storage ring energy of 2.5 GeV and a beam current between 150 and 250 mA. A Si(111) double-crystal monochromator was used for energy selection, and it was detuned by 20% at $E_0 + 50$ eV to suppress higher harmonic radiation; resolution, $\Delta E/E$, was estimated to be 2.0×10^{-4}. The transmission measurement geometry was arranged using gas-filled ionization chambers to monitor the intensities of the incident and transmitted X rays. In order to gain the proper absorption ratio for the incoming X rays, the gas compositions in the ionization chamber were selected as argon 3 mL/min with nitrogen 60 mL/min for the first chamber and as argon 18 mL/min with nitrogen 24 mL/min for the second chamber, respectively. The monochromator was scanned in energy from 200 eV below the platinum L_{III} absorption edge (11564 eV) to 1200 eV above the edge. The catalyst samples were pressed into a self-supporting wafer with the wafer thickness chosen to give an absorbance of 2.5 and measured in a transmission mode at liquid nitrogen temperature. A standard Pt foil at room temperature was simultaneously measured as a reference so that energy calibration could be done between scans.

RESULTS

Test of sulfur poisoning catalyst deactivation. Total tetralin conversion is shown as a function of time on stream in the flow reactor (Fig. 1). At the start of a run, tetralin conversion was about 55% (turnover frequency of 0.143 s^{-1}) for both of the sulfur-poisoned catalyst samples, but after the 15-h run, it fell rapidly to about 25% (turnover frequency of 0.065 s^{-1}) for the normally sulfur-poisoned catalyst and to about 2% (turnover frequency of 0.005 s^{-1}) for the severe one. The turnover frequency was calculated on the basis of the initial Pt surface atoms (3.87×10^{-5} mol Pt/g of catalyst), measured by CO chemisorption; 0.82 moles of CO per mole of Pt were adsorbed.

As shown in Fig. 1, no significant catalyst deactivation was observed for the catalyst tested with pure tetralin, indicating that the catalyst deactivation caused by coke formation is negligible.

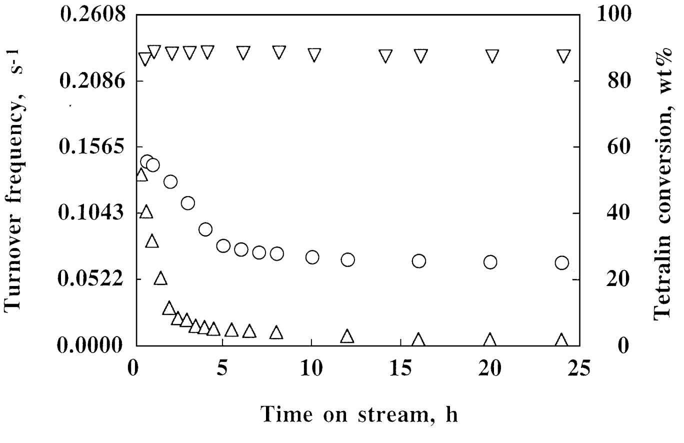

FIG. 1. Turnover frequency and tetralin conversion at 270°C; WHSV, 4.8 h^{-1}; and H_2/oil, 4.5 catalyzed by the Pt/γ-Al_2O_3 catalysts: ▽, 32 atm and 0 ppm sulfur; ○, 32 atm and 1000 ppm sulfur; △, 19 atm and 2000 ppm sulfur.

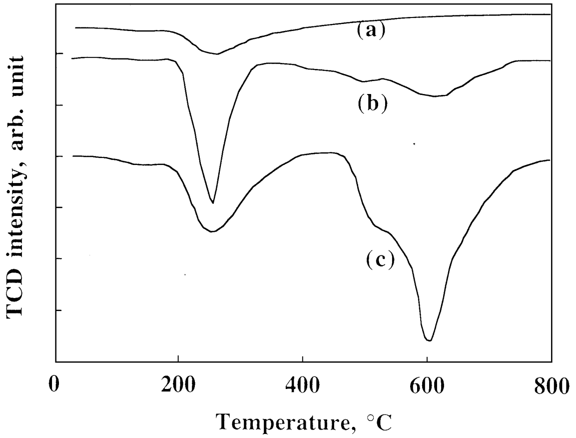

FIG. 2. Temperature-programmed reduction characterizing (a) H_2S adsorbed γ-Al_2O_3 for blank test; (b) the Pt/γ-Al_2O_3 catalyst after treatment at 270°C; WHSV, 4.8 h^{-1}; 1000 ppm sulfur; and 32 atm for 24 h (the normally sulfur-poisoned catalyst); (c) the Pt/γ-Al_2O_3 catalyst after treatment at 270°C; WHSV, 4.8 h^{-1}; 2000 ppm sulfur; H_2/Oil, 4.5; and 19 atm for 24 h (the severely sulfur-poisoned catalyst).

Temperature-programmed reduction of the sulfur-poisoned catalysts. The temperature-programmed reduction profiles characterizing the sulfur-poisoned catalyst samples are shown in Fig. 2. Peaks at 270 and 610°C with a shoulder peak at about 495°C were observed for the normally sulfur-poisoned catalyst and peaks at 300 and 605°C with a shoulder at about 535°C were observed for the severely sulfur-poisoned one. For H_2S adsorbed γ-Al_2O_3, only one peak at 260°C was observed. The negative peaks of the three samples were either resulted from the evolution of H_2S formed from the desorbed H_2S or from reduction of platinum sulfide. When the peak is not due to the desorption of adsorbed H_2S, it is a combined effect of consumption of hydrogen and the generation of H_2S from reduction of Pt sulfides. Gas chromatography with the FID detector analyzing the effluent gas indicated that no hydrocarbon was produced during the reduction process. The flame photometric detector further indicated that H_2S was the only sulfur compound in the effluent gas.

EXAFS DATA ANALYSIS

EXAFS reference data. The EXAFS data were analyzed using experimentally determined reference files obtained from standard materials of known structure. The Pt–Pt and Pt–O contributions were analyzed with phase shifts and backscattering amplitudes extracted from EXAFS data for Pt foil and $Na_2Pt(OH)_6$, respectively, and the Pt–S contribution from EXAFS data for H_2PtCl_6. The appropriateness of using the Pt–Cl to represent Pt–S is justified theoretically (17) and experimentally (14). Theoretical calculation of Teo and Lee shows that the amplitude and phase function of the nearest and next-nearest neighbors in the periodic table are hardly different (17). Moreover, for the severely sulfur-poisoned catalyst sample, the Pt–S bond length of 2.31 Å, which was estimated with Pt–Cl as a reference, is exactly the same as that for bulk PtS (24).

These three data files were provided by Dr. B. C. Gates (Department of Chemical Engineering at the University of California, Davis, CA). Details of the preparation of the reference files are described elsewhere (21).

Data analysis. A cubic spine background subtraction was used to extract EXAFS data from the measured X-ray absorption data (18). The resulting spectrum was normalized by dividing the edge height to obtain the final EXAFS functions (Fig. 3). The raw EXAFS data have a signal to noise ratio >60 for the normally sulfur-poisoned sample and >30 for both the fresh and the severely sulfur-poisoned catalyst samples. (The noise amplitude was determined at $k \cong 14$ Å^{-1}, and signal amplitude was determined at $k \cong 4$ Å^{-1}).

A k^3-weighted Fourier transformation without correction was performed on the EXAFS function over the range $2.76 < k < 14.10$ Å^{-1} for the fresh catalyst and $2.76 < k < 14.10$ Å^{-1} for the severely sulfur-poisoned catalyst; a k^2-weighted Fourier transformation was performed over the range $2.68 < k < 16.92$ Å^{-1} for the normally sulfur-poisoned catalyst. The major contributions were isolated by inverse Fourier transformation of the data in the ranges $1.08 < r < 3.25$ Å for the fresh catalyst, $1.08 < r < 3.25$ Å for the severely sulfur-poisoned catalyst, and $1.02 < r < 3.23$ Å for the normally sulfur-poisoned catalyst.

For the normally sulfur-poisoned sample, at the beginning, the coarse structural parameters characteristic of the Pt–Pt contributions were determined by fitting the k^2-weighted Fourier-isolated EXAFS function in the range $8.0 < k < 15.0$ Å^{-1}. An EXAFS function calculated from these parameters was then subtracted from the raw data (Fourier isolated EXAFS function). The residual spectra were expected to represent platinum-support interactions (Pt–O) and/or platinum–sulfur interactions (Pt–S). Since the phase functions of Pt–O and Pt–S are quite different, k^1-weighted Pt–O and Pt–Cl phase-corrected Fourier transformations were performed, respectively, on the residual EXAFS data to examine the EXAFS contributions from the backscattering atom of low atomic-number (Z). The resulting Fourier transform showed a negative peak at about 2.4 Å in r space after the Pt–O phase-corrected Fourier transformation. In contrast, for the Pt–Cl phase-corrected Fourier transformation, a positive peak appeared at about 2.3 Å with a shoulder at about 2.5 Å (Fig. 4). For an X–Y absorber-backscattering pair, peaks which have a positive imaginary part of the phase-corrected EXAFS function are due to neighbors of atom type Y (19, 20). These results thus suggest that sulfur is the low-Z backscattering atom. The structural parameters of this contribution were then estimated by fitting the k^3-weighted residual data in the range $3.5 < k < 12$ Å^{-1}. The Pt–S contribution was subtracted from the data, and better parameters for the Pt–Pt contribution were estimated. This process was repeated, and the final parameters of Pt–S and first shell Pt–Pt contribution (peaking at about 2.7 Å) were obtained from the fitting of the raw data by a nonlinear least-square multiple-shell fitting routine (18, 20, 21).

The structural parameters of the fresh and severely sulfur-poisoned catalysts were directly determined by a nonlinear least-square multiple-shell fitting routine with the high-Z (Pt) and low-Z (O and S) contributions. Further optimization of the fit was done by applying the difference file technique and phase- and amplitude-corrected Fourier

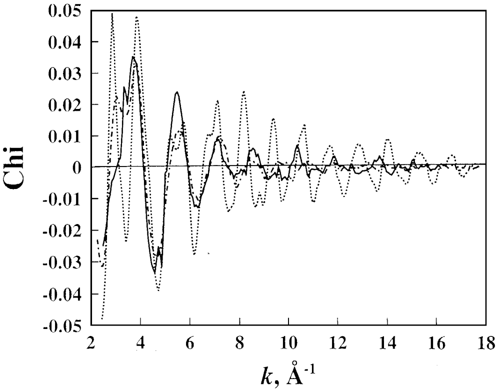

FIG. 3. Raw EXAFS data for the fresh Pt/γ-Al_2O_3 catalyst (solid line), the normally sulfur-poisoned catalyst (dotted line), and the severely sulfur-poisoned catalyst (dashed line).

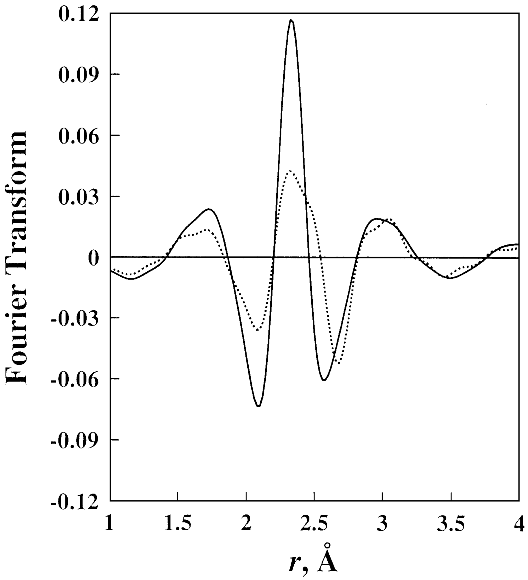

FIG. 4. Illustration of the low Z backscattering contributions for the sulfur-poisoned catalysts: imaginary part of Fourier transform (k^1-weighted, Pt–Cl phase corrected, $\Delta k = 3.50$–11.0 Å) for original filtered EXAFS data of the normally sulfur-poisoned catalyst minus calculated Pt–Pt EXAFS (dotted line) and raw EXAFS data of the severely sulfur-poisoned catalyst (solid line).

TABLE 1

EXAFS Results for the Fresh γ-Alumina-Supported Pt Catalyst[a,b,c]

Shell	N	R	$\Delta\sigma^2$	ΔE_0 (eV)	EXAFS reference
Pt–O$_{\text{(support)}}$	2.7 ± 0.3	2.15 ± 0.01	0.008 ± 0.002	−6.06	Pt–O
Pt–O$_{\text{(support)}}$	1.0 ± 0.6	2.57 ± 0.02	−0.002 ± 0.004	6.83	Pt–O
Pt–Pt	2.6 ± 0.4	2.71 ± 0.01	0.005 ± 0.001	−7.3 ± 0.7	Pt–Pt

[a] Z is the atomic number; N is the coordination number for the absorber–backscatterer pair; R, is the average absorber–backscatterer distance; $\Delta\sigma^2$ is the Debye–Waller factor; and ΔE_0 is the inner potential correction.

[b] To consider the difference of absorber–backscatterer distance between the reference shell and the Pt–Y shell to be analyzed, the coordination number N of the Pt–Y shell is corrected by the equation, $N = N_{\text{unc}}\, e^{2(R_{\text{j}} - R_{\text{ref}})/\lambda(k)}$, where N_{unc} is determined in the EXAFS data analysis by using R_{ref} as a reference coordination distance.

[c] The number of parameters used to fit the data in this first shell is 12; the statistically justified number is approximately 17, estimated from the Nyquist theorem, $n = (2\Delta k \Delta r/\pi) + 1$ (36), where Δk and Δr, respectively, are the k and r ranges used in the forward and inverse Fourier transform.

transforms (20). The resulting coordination parameters and the corresponding standard deviations are summarized in Table 1 for the fresh catalyst, in Table 2 for the normally sulfur-poisoned catalyst, and in Table 3 for the severely sulfur-poisoned catalyst. The comparisons of the data with the fit, both in k space and in r space, are shown in Figs. 5, 6, and 7, respectively, for the fresh, normally sulfur-poisoned, and severely sulfur-poisoned catalysts.

DISCUSSION

Evidence of sulfur poisoning induced Pt agglomeration. After the normally sulfur-poisoning catalyst deactivation test, the Pt–Pt first shell coordination number increased from 2.6 to 7.3, indicating the increasing size of Pt clusters. A Pt–Pt first shell coordination number of 2.6 for the fresh catalysts represents an average particle size of about 5.5 Å containing four platinum atoms. The platinum clusters of the normally deactivated catalyst contains both sulfided and unsulfided Pt clusters. EXAFS can only measure the size of unsulfided Pt clusters but not sulfided Pt clusters. On the other hand, transmission electron microscopy (TEM) cannot distinguish sulfided and unsulfided Pt clusters and measures the average Pt size of both types of Pt clusters. The average unsulfided platinum clusters of the normally deactivated catalyst contains about 85 atoms and is about 13.8 Å, estimated from the Pt–Pt first shell coordination number (22). The average Pt particle size, measured by TEM, is about 40 Å. Besides an increase of the Pt–Pt coordination number after sulfur poisoning, an increase of the average Pt–Pt bond distance from 2.72 to 2.78 Å and a decrease of the Debye–Waller factor from 0.0046 to 0.0001 are consistent with the growth of platinum clusters.

TABLE 2

EXAFS Results for the Normally Sulfur-Poisoned Pt Catalyst[a,b,c]

Shell	N	R	$\Delta\sigma^2$	ΔE_0 (eV)	EXAFS reference
Pt–Pt	7.3 ± 0.2	2.779 ± 0.001	0.0001 ± 0.0002	−4.0 ± 0.2	Pt–Pt
Pt–S	1.9 ± 0.5	2.34 ± 0.03	0.008 ± 0.005	−4.06	Pt–Cl
Pt–S	0.5 ± 0.4	2.53 ± 0.02	−0.004 ± 0.004	−5.06	Pt–Cl

[a,b] All footnotes are the same as in Table 1.

[c] The number of parameters used to fit the data in this first shell is 12; the statistically justified number is approximately 20.

TABLE 3

EXAFS Results for the Severely Sulfur-Poisoned Pt Catalyst[a,b,c]

Shell	N	R	$\Delta\sigma^2$	ΔE_0 (eV)	EXAFS reference
Pt–S	2.72 ± 0.07	2.310 ± 0.003	0.0039 ± 0.0004	0.6 ± 0.4	Pt–Cl

[a,b] All footnotes as in Table 1.

[c] The number of parameters used to fit the data in this first shell is 4; the statistically justified number is approximately 17.

Structure of the sulfur-poisoned catalysts. According to van Zon (23), the Pt–Pt bond distance of 3.9 Å, which is the second Pt–Pt coordination shell of Pt atoms in the face-centered-cubic (fcc) structure, is an indication of the three-dimensional character of the metal clusters. For the normally sulfur-poisoned catalysts, a peak was observed in this region, as shown in Fig. 8, indicating that the growth of Pt clusters occurred in three dimensions. Furthermore, the higher-shell data provide information about platinum particle morphology. The comparison of the locations of the higher-shell peaks in Fig. 8 shows that the peaks characterizing the Pt–Pt contributions of the normally sulfur-poisoned catalysts are located at the same positions as those characteristic of Pt foil. The results demonstrate that the unsulfided platinum atoms within the Pt particles form a 3-dimensional layer with the structure strongly resembling the fcc structure characteristic of Pt foil.

The Pt–Cl phase-corrected Fourier transformation of the residual EXAFS data from the subtraction of the Pt–Pt contribution from the raw data (Fourier isolated data) of the normally sulfur-poisoned catalysts showed a positive peak at about 2.3 Å with a shoulder at about 2.5 Å (Fig. 4). Using the difference file technique, this residual data was decoupled into two Pt–S contributions with bond distances at 2.34 and 2.53 Å. The peak at 2.34 Å is close to the Pt–S bond distance of bulk PtS (2.31 Å) (14, 24), and the results suggest the formation of bulk PtS during the sulfur poisoning tests. The peak at 2.53 Å is about 0.13 Å longer than the bond distance of PtS_2 (2.40 Å) (14, 25, 26), which has a structure similar to the hexagonal layer-lattice CdI_2. The peak

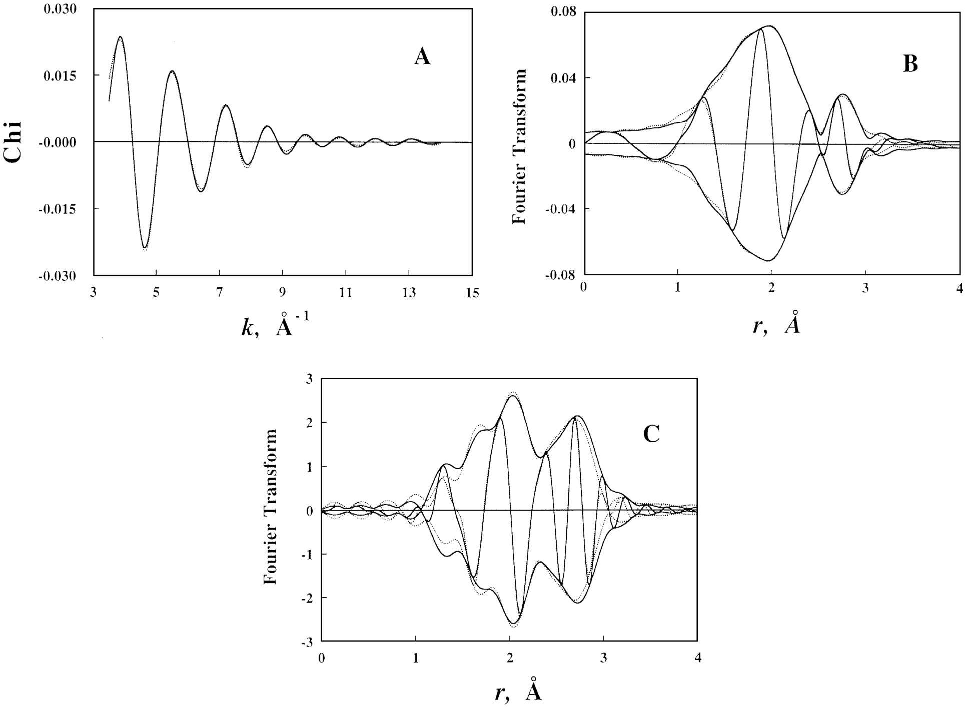

FIG. 5. Results of EXAFS analysis obtained with the best fitted structural parameters for the fresh Pt/γ-Al_2O_3 catalyst: A, k^0-weighted experimental EXAFS (solid line) and sum of the calculated Pt–Pt plus two Pt–O contributions (dashed line); B, imaginary part and magnitude of Fourier transform (k^1-weighted, $\Delta k = 3.5$–13.0 Å) of experimental EXAFS (solid line) and sum of the calculated Pt–Pt plus two Pt–O contributions (dashed line); C, imaginary part and magnitude of Fourier transform (k^3-weighted, $\Delta k = 3.5$–13.0 Å) of experimental EXAFS (solid line) and sum of the calculated Pt–Pt plus two Pt–O contributions (dashed line).

at 2.53 Å might thus be assigned as the adsorption of H_2S on platinum particles.

According to the report of Vaarkamp *et al.*, for a sulfur-poisoned Pt/BaK-LTL catalyst, the sulfur is located at the platinum–zeolite interface, inferred from the weakened Pt–O (support oxygen) contribution of the catalyst after H_2S adsorption (14). Our experimental results are consistent with those of Vaarkamp *et al.*; no Pt–O contributions have been observed for the sulfur-poisoned catalyst samples. Moreover, CO chemisorption measurement shows that about 0.14 mol of CO per mole of Pt was adsorbed on the normally sulfur-poisoned catalyst sample, while no adsorption CO was detected for the severely sulfur-poisoned one. The capability of CO chemisorption for the normally sulfur-poisoned catalysts may further suggest that the PtS were initially formed at the Pt–alumina interface and that the unsulfided Pt atoms are present in a layer with fcc structure atop the PtS layer.

The EXAFS results demonstrate that after the severe sulfur poisoning, only clusters with the morphology closely resembling bulk PtS were formed on the surface, as indicated by the Pt–S contribution of bond distance 2.31 Å (Fig. 4, Table 3).

Temperature-programmed reduction of the sulfur-poisoned catalysts. The sulfur-poisoned catalysts were also characterized by TPR, and the results are shown in Fig. 2. Since H_2S was the only species detected in the effluent gas during the TPR measurement, the TPR peaks were regarded as the results of the reduction of platinum sulfide and/or the desorption of the adsorbed H_2S. The possibility of benzothiophene adsorbed on the catalyst has also been ruled out, because no reaction products such as styrene and ethylbenzene were detected in the effluent gas during the TPR measurement.

In comparison with the TPR peak of the H_2S adsorption on γ-alumina sample, the TPR peak at 290°C for the severely sulfur-poisoned catalyst and 270°C for the normally sulfur-poisoned one may be assigned as the characteristic peaks of the desorption of H_2S on the γ-alumina support; the H_2S desorption peak of the γ-alumina sample (Fig. 2) is at 265°C.

In this study, the purpose of TPR characterizing the H_2S adsorbed γ-alumina sample was to determine the desorption temperature of H_2S on γ-alumina. Adsorption equilibrium of H_2S of γ-alumina was not attempted. Therefore, the smallest peak of the γ-alumina among the three samples may be due to the small amount of adsorption H_2S on the sample. However, if the TPR peak at 290°C for the severely sulfur-poisoned catalyst and 270°C for the normally sulfur-poisoned one are due to the desorption of H_2S

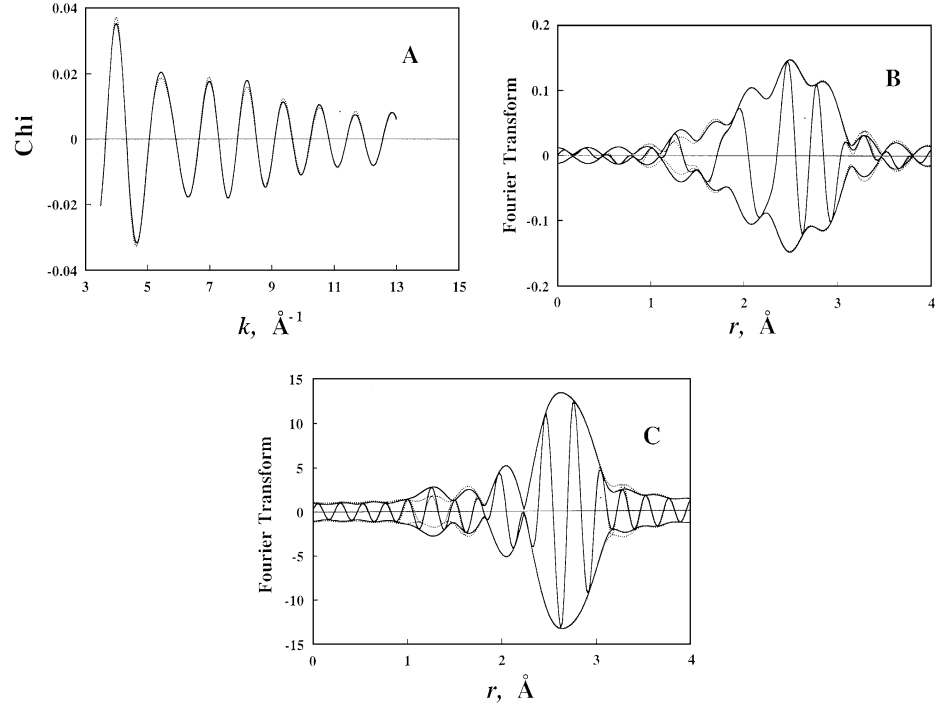

FIG. 6. Results of EXAFS analysis obtained with the best fitted structural parameters for the normally sulfur-poisoned catalyst: A, k^0-weighted experimental EXAFS (solid line) and sum of the calculated Pt–Pt plus two Pt–S contributions (dashed line); B, imaginary part and magnitude of Fourier transform (k^1-weighted, $\Delta k = 3.5$–13.0 Å) of experimental EXAFS (solid line) and sum of the calculated Pt–Pt plus two Pt–S contributions (dashed line); C, imaginary part and magnitude of Fourier transform (k^3-weighted, $\Delta k = 3.5$–13.0 Å) of experimental EXAFS (solid line) and sum of the calculated Pt–Pt two Pt–S contributions (dashed line).

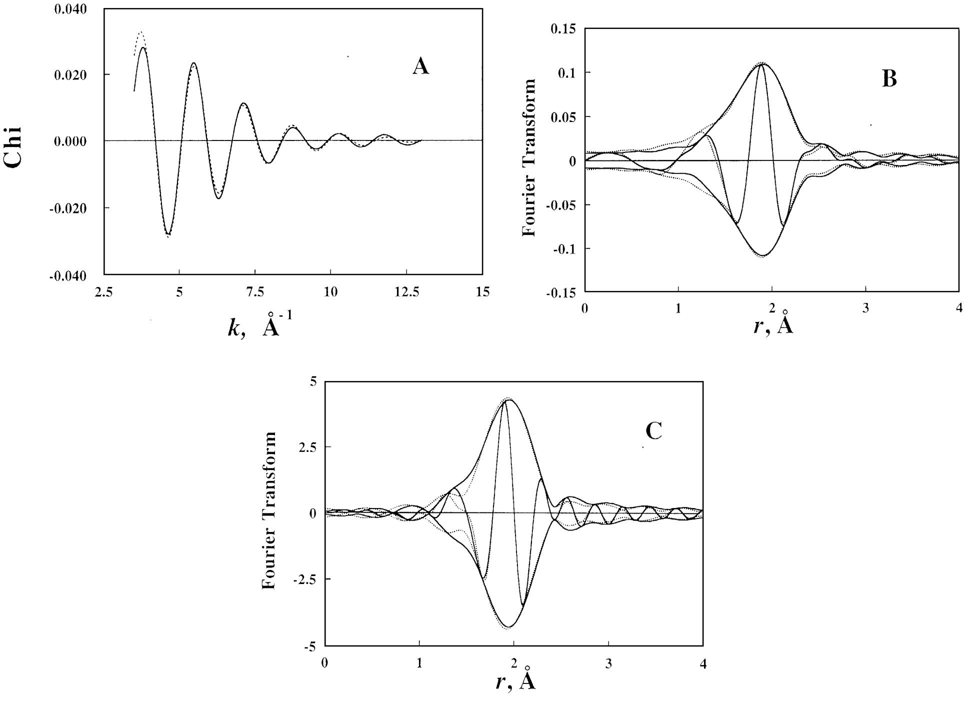

FIG. 7. Results of EXAFS analysis obtained with the best fitted structural parameters for the severely sulfur-poisoned catalyst: A, k^0-weighted experimental EXAFS (solid line) and the calculated Pt–S contribution (dashed line); B, imaginary part and magnitude of Fourier transform (k^1-weighted, $\Delta k = 3.5$–11.0 Å) of experimental EXAFS (solid line) and the Pt–S contributions (dashed line); C, imaginary part and magnitude of Fourier transform (k^3-weighted, $\Delta k = 3.5$–11.0 Å) of experimental EXAFS (solid line) and the calculated Pt–S contributions (dashed line).

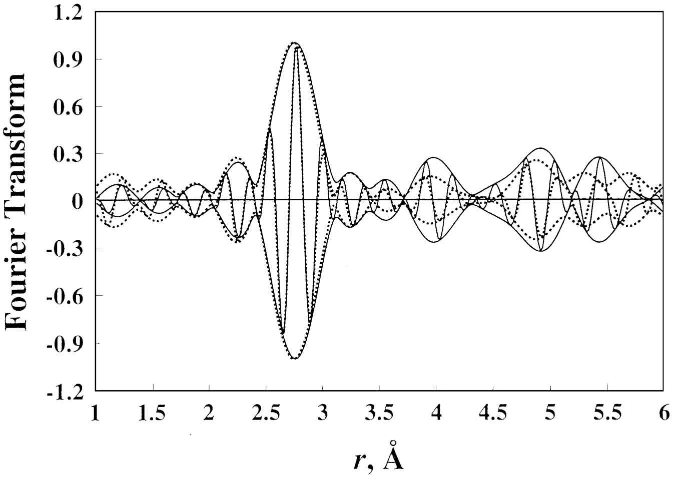

FIG. 8. Comparison of the normalized imaginary and magnitude of Fourier transforms (k^2-weighted, $\Delta k = 8.0$–17.0 Å, Pt–Pt phase, and amplitude corrected) for the Pt foil (solid line) and the normally sulfur-poisoned catalyst (dotted line).

on γ-alumina, we may expect that both catalyst samples have the same peak area. But the experimental results show that the peak area of the normally sulfur-poisoned catalyst is about 1.35 times that of the severely sulfur-poisoned one. Therefore, it is concluded that other plausible assignments such as the desorption of H_2S from Pt clusters may not be ruled out.

Since the coordination number of the PtS is greater than that of the chemisorbed H_2S, the peak at 600°C for the normally sulfur-poisoned catalysts might be assigned as the reduction of bulk PtS and the shoulder peak at 495°C as the desorption of the chemisorbed H_2S or the "irreversible" adsorbed H_2S (27–29); the alumina adsorbed H_2S that does not exist on pure alumina but interacts with the metal was noted as "irreversible" adsorbed H_2S.

Similarly, for the severely sulfur-poisoned catalyst samples, the peak at 605°C might be assigned as the reduction of the bulk PtS and the small shoulder at 535°C as the desorption of the chemisorbed H_2S on PtS.

Mechanism of sulfur-induced metal agglomeration. Two Pt–O distances were observed for the fresh catalyst: one at 2.17 Å and one at 2.64 Å. The shorter Pt–O distance of 2.17 Å has been suggested to be characteristic of the interaction between metals to the right of W in the periodic table and oxygen of nonreducible metal oxide supports. The longer distance is suggested to be due to the interaction between platinum and surface oxygen with the presence of hydrogen between the platinum clusters and γ-Al_2O_3 support (30). After the sulfur poisoning tests, no Pt–O contributions were observed; the EXAFS contributions of the interactions between platinum clusters with the surface oxygen may be so small that they are covered by noise. Instead, concomitant with the formation of PtS, a migration of Pt particles was observed by EPMA characterizing Pt concentration profiles of the catalysts (13).

Together with the EPMA, TPR, and EXAFS results, we might speculate on the mechanism of sulfur-poisoning-induced Pt agglomeration from the evidence of the adsorption of H_2S on the alumina support, the loss of the metal–support interaction, and the migration of Pt clusters during sulfur poisoning.

The oxygen of γ-Al_2O_3 support may be viewed as rigid ligands that bond with Pt clusters so as to inhibit their migration. If the affinity of Pt for H_2S is greater than that for the surface oxygen, H_2S may replace the surface oxygen and loosen the interaction of the Pt clusters with the support. During sulfur poisoning, the H_2S adsorbed on γ-Al_2O_3 may diffuse to the Pt–alumina interface and react with Pt to form platinum sulfides. Concomitant with the formation of platinum sulfides, the adsorbed H_2S decreases the Pt–alumina interaction and thus promotes migration of platinum clusters, leading to a growth of platinum particle size and to a loss of catalyst activity.

The Pt agglomeration during sulfur poisoning can also be explained by the formation of platinum sulfides via the direct reaction of H_2S with the Pt clusters. Since platinum sulfides melting point is much lower than Pt and also has much higher vapor pressure and therefore is much easier to agglomerate. The fraction of the Pt atoms in contact with the support would decrease with the growth of platinum particle size, leading to a decrease of Pt–O contributions; platinum–oxygen$_{\text{support}}$ interaction may exist in the normally sulfur-poisoned catalyst, but it may be too small to be analyzed.

According to the report of Cooper *et al.* (11), the sulfur resistance of a noble metal can be enhanced by utilizing acidic support, such as acidic zeolites and amorphous silica–aluminas. The consensus regarding the role of the acidic support is that the interaction between acidic sites of the support and the small Pt clusters decreases the electron density of Pt and, thus, lowers the bond strength between the electron acceptor (H_2S) and the electron deficient Pt particles (11, 31, 32). As the model described, the only role of acidic support is to modify the Pt sites so as to inhibit the adsorption of H_2S. However, based on the proposed mechanisms for Pt agglomeration induced by sulfur poisoning, the increase of support acidity may decrease the formation rate of platinum sulfides and/or inhibit the adsorption of H_2S on the support, thereby retarding the Pt agglomeration rate. In contrast, a basic support enhances Pt agglomeration. As indicated by Vaarkamp *et al.* (14), the high sensitivity of the Pt/BaK–LTL catalyst to poisoning by very low levels of sulfur is attributed to the loss of active platinum surface by the adsorption of sulfur and the growth of the platinum clusters.

To enhance the sulfur resistance of a supported Pt catalyst so the catalytic activity improves for aromatics reduction, extensive research has been undertaken on the sulfur poisoning catalyst deactivation. However, most of the researchers are only concerned about the catalyst deactivation caused by the adsorption of H_2S on Pt particles and the formation of platinum sulfides. Therefore, the interactions between Pt and H_2S attract the most attention of the researchers (4, 11, 33). From industrial aspects, to remove the adsorbed H_2S on Pt and to reduce PtS by hydrogen reactivation is relatively easier than to restore the original particle size of a supported Pt catalyst by the oxylchlorination method (13, 34, 35). Research in the area of finding a doping element to reduce the tendency of Pt to chemisorb H_2S or forming bulk sulfide is important for the improvement in sulfur resistance of a Pt catalyst.

CONCLUSIONS

X-ray absorption and TPR were used to characterize the structure of the fresh and sulfur-poisoned Pt/γ-Al_2O_3 catalysts. The experimental results indicate that sulfur poisoning induces a morphology change in the Pt. The agglomeration of Pt particles may be caused by the adsorption of H_2S at the Pt–alumina interface leading to a decrease of Pt–support interactions and/or the direct reaction of H_2S with Pt leading to the formation of relatively mobile platinum sulfides. The agglomeration of Pt particles makes the regeneration of the sulfur-poisoned catalysts more difficult; a more complicated oxylchlorination method instead is necessary to redisperse the catalysts. Therefore, to increase tolerance to sulfur poisoning, a supported Pt catalyst should be prepared with a low Pt agglomeration rate during sulfur poisoning. The choice of catalyst support and/or the finding of the second metal for the formation of bimetallic interactions so the H_2S adsorption decreases is crucial in developing high sulfur-tolerant Pt catalysts.

ACKNOWLEDGMENTS

The EXAFS data were analyzed using the XDAP Data Analysis Program, developed by M. Vaarkamp, J. C. Linders, and D. C. Koningsberger, and the reference files were provided by Dr. B. C. Gates. This research were supported by the National Science Council of the Republic of China (Contract No. NSC 85-2214-E-194-002) and by Refining & Manufacturing Research Center of the Chinese Petroleum Corp. (RMRC). We are also grateful to the staff of beam line X-11A at the National Synchrotron Light Source, U.S.A., for their assistance.

REFERENCES

1. Søgaard-Andersen, P., Cooper, B. H., and Hannerup, P. N., Topsøe's Process for Improving Diesel Quality, *Nat. Pet. Refin. Assoc. Tech. Pap.* **AM-92-50** (1992).
2. Cooper, B. H., Stanislaus, A., and Hannerup, P. N., Diesel Aromatics Saturation-A Comparative Study of Four Catalyst Systems. *Prepr. Pap. Am. Chem. Soc., Div. Fuel. Chem.* **37**(1), 41 (1992).
3. Cooper, B. H., Stanislaus, A., and Hannerup, P. N., *Hydrocarbon Process.* **June** (1993).
4. Barbier, J., Lamy-Pitara, E., Mareccot, P., Boitiaux, J. P., Cosyns, J., and Verna, F., *Adv. Catal.* **37**, 279 (1990).
5. Suchanek, A. J., *Oil Gas J.* **May** (1990).
6. Kukes, S. G., Clark, F. T., Hopkins, D. P., and Green, L. M., U.S. Patent 5,308,814 (1993).
7. Kovach, S. M., and Wilson, G. D., U.S. Patent 3,943,053 (1976).
8. Minderhoud, J. K., and Lucien, J. P., U.S. Patent 4,960,505 (1988).
9. Kukes, S. G., Clark, F. T., Hopkins, D. P., and Green, L. M., U.S. Patent 5,151,172 (1992).
10. Kukes, S. G., Clark, F. T., Hopkins, D. P., and Green, L. M., U.S. Patent 5,271,828 (1993).
11. Cooper, B. H., and Donnis, B. B. L., *Appl. Catal. A: Gen.* **137**, 203 (1996).
12. Lin, T.-B., Jan, C.-A., and Chang, J.-R., *Ind. Eng. Chem. Res.* **34**, 4284 (1995).
13. Chiou, J.-F., Huang, Y.-L., Lin, T.-B., and Chang, J.-R., *Ind. Eng. Chem. Res.* **34**, 4277 (1995).
14. Vaarkamp, M., Miller, J. T., Modica, F. S., Lane, G. S., and Kiningsberger, D. C., *J. Catal.* **138**, 675 (1992).
15. Gates, B. C., Katzer, J. R., and Schuit, G. C. A., "Chemistry of Catalytic Process," p. 396. McGraw–Hill, New York, 1979.
16. Jones, A., and McNicol, B., "Temperature-Programmed Reduction for Solid Materials Characterization," p. 70. Dekker, New York, 1986.
17. Teo, B. K., and Lee, P. A., *J. Am. Chem. Soc.* **101**, 2815 (1979).
18. van Zon, F. B. M., "A Structural Investigation of Supported Small Metal Particles and the Metal–Support Interface with EXAFS," p. 18. Dissertation, Eindhoven University of Technology, Eindhoven, The Netherlands, 1988.
19. Lee, P. A., and Beni, G., *Phys. Rev. B* **15**, 2862 (1977).
20. van Zon, F. B. M., Maloney, S. D., Gates, B. C., and Koningsberger, D. C., *J. Am. Chem. Soc.* **115**, 10317 (1993).
21. Kampers, F. W. H., "EXAFS in Catalysis: Instrumentation and Applications," p. 26. Dissertation, Eindhoven University of Technology, Eindhoven, The Netherlands, 1989.
22. Gates, B. C., Katzer, J. R., and Schuit, G. C. A., "Chemistry of Catalytic Process," p. 246. McGraw–Hill, New York, 1979.
23. van Zon, F. B. M., "A Structural Investigation of Supported Small Metal Particles and the Metal–Support Interface with EXAFS," p. 114. Dissertation, Eindhoven University of Technology, Eindhoven, The Netherlands, 1988.
24. Heegemann, W., Meister, K. H., Bechtold, E., and Hayek, K., *Surf. Sci.* **49**, 161 (1975).
25. Greenwood, N. N., and Earnshaw, A., "Chemistry of the Elements," p. 803. Pergamon, Elmsford, NY, 1984.
26. Demuth, J. E., Jepsen, D. W., and Marcus, P. M., *Phys. Rev. Lett.* **32**, 1182 (1974).
27. Apesteguia, C. R., Barbier, J., Plaza de los Reyes, J. F., Garetto, T. F., and Parera, J. M., *Appl. Catal.* **1**, 159 (1981).
28. Apesteguia, C. R., Barbier, J., Plaza de los Reyes, J. F., and Garetto, T. F., *React. Kinet. Catal. Lett.* **15**, 167 (1980).
29. Barbier, J., Marecot, P., Tifouti, L., Guenin, M., and Frety, R., *Appl. Catal.* **19**, 375 (1985).
30. Koningsberger, D. C., and Gates, B. C., *Catal. Lett.* **14**, 271 (1992).
31. Dalla Betta, R. A., and Boudart, M., "Proceedings, 5th International Congress on Catalysis, Palm Beach, 1972" (J. W. Hightower, Ed.), Vol. 2, p. 1329. North Holland, Amsterdam, 1973.
32. Gallzot, P., Dakta, J., Massardier, M., Primat, M., and Imelik, B., "Proceedings, 6th International Congress on Catalysis, London, 1976" (G. C. Bond, P. B. Wells, and F. C. Tompkins, Eds.), Vol. 2, p. 696. The Chemical Society, London, 1977.
33. Stanislaus, A., and Cooper, B. H., *Catal. Rev.-Sci. Eng.* **36**(1), 75 (1994).
34. Hoyos, L. J., Primet, M., and Praliaud, H., *J. Chem. Soc. Faraday Trans.* **88**(22), 3367 (1992).
35. Fung, S. C., *CHEMTECH* **January**, 40 (1994).
36. Koningsberger, D. C., and Prins, R., "X-Ray Absorption: Principles, Applications, Techniques of EXAFS, SEXAFS, and XANES," p. 395. Wiley, New York, 1988.